Temperature Dependence of Kinetic Isotope Effects for Enzymatic Carbon−Hydrogen Bond Cleavage

Willem Siebrand* and Zorka Smedarchina

Steacie Institute for Molecular Sciences, National Research Council of Canada, Ottawa, K1A 0R6 Canada

Received: May 7, 2003; In Final Form: December 1, 2003

An analysis is reported of the anomalously weak temperature dependence of large kinetic isotope effects (KIEs) observed for enzymes that catalyze carbon−hydrogen bond cleavage. After a critical examination of the experimental data, rate expressions for proton tunneling are used to derive a universal relationship between KIEs and their temperature dependence for a model in which the tunneling coordinate, represented by two crossing Morse potentials or a quartic double-minimum potential, is assisted by a harmonic promoting mode. Since the reactions involve electron transfer to a redox system as well as proton transfer from a CH to an OH bond, both adiabatic and nonadiabatic mechanisms are considered. Model calculations are reported, which show that the derived relationship is valid under a wide range of conditions and depends on a minimum number of model parameters, namely almost exclusively on the proton transfer distance and the tunneling-mode anharmonicity. The results are used to derive proton transfer distances and promoting-mode force constants from the available data on temperature-dependent isotope effects for several enzymatic reactions effecting CH cleavage, including the reactions of linoleic acid catalyzed by soybean lipoxygenase-1 (SLO1), of primary amines catalyzed by methylamine and aromatic amine dehydrogenase (MADH and AADH), and of a dicopper complex that models the active site of monooxygenases and lacks a protein environment. These distances are found to be shorter and the force constants to be larger than those implied by van der Waals radii, but with anharmonicities suitably adjusted, they resemble those encountered in systems with hydrogen bonding. It is proposed that the strong redox system, which is always present in these enzymes, acts so as to withdraw electron density from the C···H···O transfer system. This will tend to shrink the tunneling barrier to a size that allows effective passage of H but not necessarily of D, a condition that may lead to a large KIE. It will also increase the enzyme−substrate force constant, thus reducing the temperature dependence of the KIE. For the reaction catalyzed by SLO1, a transfer distance of 0.9−1.0 Å is found. Similar results are obtained for three artificial mutants from which it is concluded that parts of the protein located outside the reaction site have little influence on the proton transfer. For the reactions catalyzed by MADH and AADH, the corresponding values range from 0.5 to 1.0 Å; however, the values much below 1.0 Å may be unrealistic since they are based on data that show anomalies suggesting that an incomplete kinetic model was used in their derivation. The analysis also yields a transfer distance of about 0.9 Å for the dicopper complex, a value similar to that of SLO1, although no protein is present. Since results for three different systems cluster about the same transfer distance of 0.9−1.0 Å, it is concluded that the large KIEs and their weak temperature dependence are due to a redox-induced C···H···O hydrogen bond.

1. Introduction

Certain enzymes are observed to exhibit a strongly reduced reactivity if the substrate is deuterated at a carbon atom.[1−8] This reduction, typically by a factor of 10−100, is usually interpreted as evidence for a rate-determining hydrogen tunneling step. From a biological point of view, such an observation is not surprising since deuterated substrates are not normally present in concentrations that may endanger the proper functioning of organisms, so that there is no evolutionary bias against mechanisms relying on quantum-mechanical tunneling. On the contrary, since tunneling increases the catalytic efficiency of the enzyme, it is to be expected to be a prominent feature in enzymatic processes. If the hydrogen is transferred along a hydrogen bond, the kinetic isotope effect (KIE), defined as the ratio of hydrogen and deuterium rate constants, is usually fairly small at biologically relevant temperatures, since hydrogen bonding leads to short tunneling distances, but if the transfer involves a hard-to-break carbon−hydrogen bond that is not involved in hydrogen bonding, it may be expected to be large. This provides the investigator with a powerful tool for analyzing enzymatic reaction mechanisms. However, to go beyond the simple observation that tunneling is a rate-determining step, and to discriminate between different reaction pathways, we need a quantitative understanding of the nature of these isotope effects.

In an effort to obtain such an understanding, several investigators have studied the temperature dependence of the KIE in the narrow range of temperatures near room temperature where these systems are stable.[1−7] In a number of cases, notably reactions catalyzed by soybean lipoxygenase-1 (SLO1)[3,4] and by methylamine dehydrogenase (MADH) and aromatic amine hydrogenase (AADH),[5−7] it was found that the KIE is almost independent of temperature. This is an anomalous result in that it contradicts not only presently available theoretical models but also disagrees with observations made on a wide variety of nonenzymatic systems. While the hydrogenic vibrations that govern tunneling may have too high a frequency to be thermally

* To whom correspondence should be addressed.

10.1021/jp030575t CCC: $27.50
Published on Web 03/04/2004

excited at room temperature, modern tunneling treatments recognize the contributions of low-frequency modes to the transfer. These modes may help or hinder tunneling but all theories agree that at higher temperatures they help more and hinder less. Since such modes are always present, the only way to make their contribution temperature-independent is to assign high frequencies to them. This in turn implies a steep potential and thus a short distance between the groups exchanging the hydrogen.

In this paper, we propose to address the problem of the weak temperature dependence of several enzymatic KIEs, first, by critically examining the experimental evidence and, second, by studying general theoretical models that focus on KIEs rather than rate constants so as to minimize the parameter dependence of the results. Our ultimate aim is to formulate a specific mechanism for the rate-determining steps of these reactions. First we note that the enzymatic reactions for which these anomalous KIEs are observed share certain characteristics. They generally involve cleavage of a carbon−hydrogen bond. This is a difficult and, therefore, relatively slow process, requiring a powerful catalyst. The catalytic step involves the transfer of an electron as well as that of a proton. Direct comparison with a reaction that is not catalyzed is not possible since uncatalyzed hydrogen transfer reactions leading to CH-bond cleavage usually involve either free radicals or excited states. It thus appears that electron transfer plays the same part in enzymatic CH-bond cleavage as electronic excitation or radical formation in uncatalyzed reactions. Electron transfer can promote cleavage in two different ways, namely by driving a *simultaneous* proton-transfer process or by forming a stable zwitterionic intermediate that allows a *subsequent* proton transfer process. In the absence of any direct evidence for such an intermediate, the former alternative, implying nonadiabatic proton transfer, seems to be generally favored over the latter, adiabatic process.

Hydrogen tunneling in the presence of a complex environment such as would apply to enzyme catalysis was addressed recently by Antoniou and Schwartz,[9] who analyzed the way presently available theories treat the interaction of the proton motion and the substrate vibrations, but did not discuss transfer distances. In a later study Kuznetsov and Ulstrup[10] presented an analysis of the SLO1 data of ref 3 and recognized that these data imply a tunneling distance much shorter than that deduced from van der Waals radii. Their approach forms the basis for the recent attempt by Knapp et al.[4] to model the temperature dependence of the KIE of SLO1. The authors assumed nonadiabatic proton transfer and arrived at a transfer distance of about 0.6−0.7 Å, a value about half that estimated on the basis of the van der Waals radii of the methylene and hydroxyl groups between which the transfer occurs. Since methylene groups are not normally engaged in hydrogen bonding to hydroxyl groups, this may suggest that the short distance is due to a hitherto unknown type of protein dynamics resulting in "squeezing" of the active site by the protein. However, proteins, which consist of flexible strands held together by relatively weak hydrogen bonds, would appear to be ill-equipped to cause strong local compression. To overcome the repulsion generated by shortening the methylene−hydroxyl distance by about 0.6 Å, several new hydrogen bonds would be required in locations such that the flexibility of the enzyme−substrate complex would be severely restricted at the active site. Since the substrate, linoleic acid, is relatively large and flexible, with a polar group well away from the active site, it is difficult to see how this could be accomplished.

A further argument against nonlocal protein effects on proton tunneling is the observation of CH-cleavage reactions with temperature-dependent KIEs similar to those in enzymes in model compounds outside a protein environment. One of these, which we include in our study, takes place in a bound dicopper complex that has been used as a model for reactions catalyzed by monooxygenases.[11] The temperature-dependent KIEs reported for the complexes are large but show a weak temperature dependence, comparable to those obtained for SLO1.

In this contribution, we aim to analyze reported kinetic data for reactions of this type in terms of a general tunneling approach that is simple enough to allow investigation of a large set of such data without requiring a large number of parameters. The approach we adopt, based on our previous work on simple organic systems,[12−14] uses both the Golden Rule of time-dependent perturbation theory to treat proton transfer as a nonadiabatic transition between two diabatic surfaces and modern quasiclassical theories to treat proton transfer on a single adiabatic surface.[15] The Golden Rule approach, which is always possible if the perturbation causing the transition is time-independent, starts with a division of the Hamiltonian of the system into a zeroth-order term and a perturbation, such that the process can be described as a transition between two eigenstates of the zeroth-order term driven by the perturbation. It is particularly apt if the perturbation is weak, so that it only causes transitions but does not distort the diabatic potentials near equilibrium, which can then be represented by standard adiabatic potentials in the initial and final equilibrium configurations. The Golden Rule can still be used if the perturbation is strong provided the potentials are properly modified. For the present system this description implies simultaneous electron−proton transfer; the standard Golden Rule expression appears after integration over the electronic coordinates. An advantage of this approach is that it avoids the problem of evaluating the transition state and barrier height; instead, the transition rate is described entirely in terms of equilibrium configurations. A disadvantage is that it is difficult to define the perturbation and hence to evaluate rate constants quantitatively. The Golden Rule approach is not suitable for short transfer distances and low barriers. To cover these situations, we use a method based on the instanton approach.[15] Our approximate instanton method describes the passage of the proton through a barrier constructed from a single adiabatic surface but modified so as to include the effects of all vibrations that can influence the rate of passage. In principle, the question of the simultaneity of the electron and proton transfer can be settled by a quantum-chemical evaluation of the required potential-energy surface. Unfortunately, this is not feasible at the present time. In the absence of any experimental information concerning the presence or absence of an intermediate state, we choose an empirical approach that does not rely on this information.

We begin our study with a critical examination of the reported "anomalous" enzymatic KIE data. We then use the Golden Rule approach to derive a relationship between the magnitude of the KIE and its temperature dependence that can be used to analyze the proton transfer mechanism. We develop this relationship for a simple model that can be solved analytically and subsequently probe its accuracy by numerically solving a more elaborate model. After showing how the results can be generalized to systems outside the range of the Golden Rule, we apply them to a number of enzymatic proton-transfer reactions.

2. CH-Bond Cleavage by Lipoxygenase

To analyze the basic mechanism of the electron + proton transfer step common to the reactions to be considered, we start with the reaction catalyzed by lipoxygenase for which the active

site of the enzyme is well-characterized and relatively simple. The analysis is based on data obtained from a study of SLO1 carried out recently by Klinman et al.[3,4] These data concern the rate of hydrogen abstraction from the C-11 methylene group of linoleic acid. The authors measured rate constants in the temperature range 278−323 K for linoleic acid and two isotopomers, namely 11-(S)-[^{2}H] and 11,11-[$^2H_2$] linoleic acid, obtaining values $k_{cat} = 3-300\ s^{-1}$ and KIEs of about 80. Both the rate constants and the KIEs showed a weak temperature dependence in this range. The study also included SLO1 mutants in which a bulky amino acid near the active site was replaced by alanine. Two of these mutants showed a strongly reduced activity, whereas the third showed little difference from the wild-type enzyme. All three mutants showed KIEs similar to that of SLO1, but with a somewhat stronger temperature dependence.

Lipoxygenase is a metallo-enzyme containing a six-coordinated iron that alternates between Fe(III) and Fe(II) during the catalytic cycle. The proposed first step in the cycle is one-electron oxidation by Fe(III)OH accompanied by proton transfer to yield a delocalized radical and Fe(II)OH_2. A 1.4 Å X-ray structure is available of the enzyme without the substrate.[16] The probable location of the substrate, linoleic acid, in one of the available pockets inside the protein has been identified, but the exact position of the methylene group (C-11) remains unknown. Although this uncertainty combined with the complexity of the active site renders a detailed quantum-chemical study impractical at this time, the basic steps involved in the transfer mechanism are well-known.

The reactant we represent symbolically by

$$-C{=}C-CH_2-C{=}C- + Fe(III)OH \qquad (\mathbf{I})$$

and the product by

$$-C{=}C-\dot{C}H-C{=}C- + Fe(II)OH_2 \qquad (\mathbf{II})$$

This reaction can be viewed as electron plus proton (not electron plus hydrogen) transfer. Electron transfer without proton transfer would lead to a structure of the form

$$-C{=}C-CH_2^{+}-C{=}C- + Fe(II)OH^{-} \qquad (\mathbf{III})$$

whereas proton transfer without electron transfer would yield

$$-C{=}C-CH^{-}-C{=}C- + Fe(III)^{+}OH_2 \qquad (\mathbf{IV})$$

We expect that structure **III** has a stable local minimum along the proton coordinate; the proposed simultaneous transfer of the proton would imply that it has a higher energy than structure **I**. Thus, if **I** is the ground state of the reactant, **III** is an excited state. Similar arguments suggest that **II** is the ground state of the product and **IV** an excited state. It follows that along the hydrogen-transfer coordinate, with the electron left on the substrate, **I** correlates with **IV** and, with the electron transferred to the enzyme, **II** correlates with **III**. Representing each correlated pair by a double-minimum potential along −C···H···O−, we obtain a diagram in which two such potentials, each with its own transition state, will cross somewhere near the center of the coordinate. This crossing will be avoided if the potentials interact along this coordinate, which they will generally do if there are no symmetry restrictions. If the interaction is strong, the crossing will be strongly avoided, so that the resulting upper and lower branches remain well separated. We can then limit our treatment of the hydrogen transfer to the lower branch, the maximum of which will constitute a third transition state, but it is clear that the presence of three transition states would greatly complicate the quantum-chemical analysis. If the interaction is weak compared to vibrational frequencies, the transfer will be essentially nonadiabatic, so that its rate constants can be evaluated by the Golden Rule from the known properties of CH and OH oscillators. This is basically the approach adopted in ref 4.

A different approach was taken by Tresadern et al.,[17] who treated the tunneling as an adiabatic process, thus implicitly assuming strong coupling between the electronic states associated with the electron transfer. Using a PM3/d potential and replacing linoleic acid by 1,4-pentadiene, they calculated transfer rate constants for neutral hydrogen and deuterium atom transfer by transition state theory with semiclassical tunneling corrections in the small-curvature approximation.[18] However, these calculations did not reproduce the observed large KIE and did not address the problem of the weak temperature dependence of the KIE.

The model of ref 4 is based on a low-order perturbation approach in which the two vibrational potentials involved in proton-transfer belong to different electronic manifolds related by electron transfer. In lowest order, the coupling between these manifolds causes proton transfer. Higher-order effects leading to distortion of the vibrational potentials are neglected. Since the potentials are assumed harmonic, the barrier resulting from their crossing will be very high if a normal, i.e., van der Waals type, separation is assumed. To account for the observed temperature dependence of the KIE in this harmonic model, a much smaller separation is required. The harmonic approximation is unrealistic, as the authors[4] realized, but might be partially justified by the assumption that the protein compresses the active site strongly enough to overcome the repulsion, since the compression will tend to reduce the anharmonicity of the CH- and OH-stretching vibrations involved in the proton transfer. However, since the forces required to overcome the repulsion will distort the potentials in a way that reduces their interaction, such a mechanism is basically inefficient and thus unlikely to evolve naturally.

Reducing the distance in order to enhance tunneling will be most effective if accompanied by enhancing rather than suppressing the anharmonicity of the tunneling mode. This would require attraction rather than repulsion between the groups exchanging the proton. The structure of the active site of SLO1 suggests that this is indeed what is happening. In this and the other enzymes to be discussed, this site contains a strong redox system capable of pulling electron density away from the methylene group. One may reasonably expect this system to have a direct effect on the transfer dynamics. In terms of the nonadiabatic transfer mechanism, this means that the coupling should be strong rather than weak. Thus, starting from CH- and OH-stretching vibrations with normal anharmonicities, one expects the coupling to shorten the distance between the potentials and to increase their anharmonicity, in addition to causing transfer. In the limiting case that the redox pull leads to abstraction of a full electron prior to proton transfer, a zwitterionic hydrogen bond, stabilized by the protein, would be formed. In that case, electron−proton transfer will be essentially a two-step process. However, whether or not the electron and proton move simultaneously, the effect of the redox system on the proton-transfer potential will be in the direction of lowering the barrier, shortening the transfer distance, and stiffening the vibrations modulating this distance.

The question to be answered is whether this can account for the observed large KIE and, in particular, its weak temperature

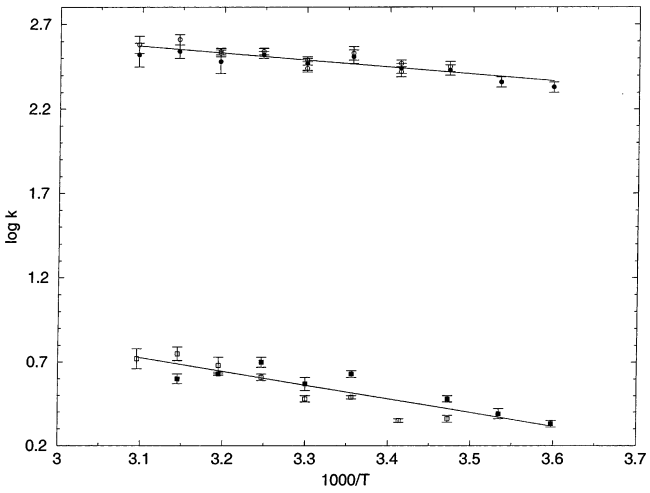

Figure 1. Combined kinetic data for the wild-type (full symbols) and I553A (open symbols) SLO1 reaction with linoleic acid for normal (circles) and dideuterated (squares) substrates, as reported in the Supplementary Material to ref 4. The solid lines represent least-squares fits with correlation coefficients 0.86/0.88 for H/D.

dependence. The magnitude of this temperature dependence is derived from that of the rate constants observed in a small temperature interval. The Arrhenius plots show considerable scatter with correlation coefficients as low as 0.84. Although this is not surprising given the complexity of the system, it means that the reported temperature dependence of the rate constants and, a fortiori, of the KIEs is subject to substantial error. The data reported in ref 4 as Supporting Information yield correlation coefficients for the Arrhenius fits of the rate constants for linoleic acid-d_0 and -d_2 of 0.90 and 0.88, respectively, and for the mutant I553A, which differs from the wild-type enzyme by a mutation that is relatively far from the reactive center, of 0.84 and 0.97, respectively. As shown in Table 1 of ref 4, this mutant shares all measured properties with the wild-type enzyme; in fact, the Arrhenius plot for the nondeuterated substrate is the same for both enzymes. It follows that the mutation concerns an amino acid that is not essential for the efficient functioning of the enzyme. Although it is claimed that for the dideuterio isotopomer the Arrhenius plots differ, the low correlation coefficients indicate that this difference is not statistically significant. This is confirmed by the observation that combining the two data sets produces correlation coefficients that represent the Arrhenius curves as well and more consistently than using these data sets separately, the corresponding values being 0.86 (instead of 0.90 and 0.84) and 0.88 (instead of 0.88 and 0.97) for the nondeuterated and dideuterated substrates, respectively. The resulting modified version of Figure 1 of ref 4 is illustrated in Figure 1. This reinterpretation confirms the general observation that two closely related compounds that show the same temperature-dependent rate constants for proton transfer also show the same temperature-dependent rate constants for deuteron transfer. It is also supported by the data set for the nondeuterated substrate reacting with the I553A mutant, since the duplicate measurements at the same temperature indicate the presence of random errors comparable or larger than the reported (presumably systematic) errors. Interpretation of the difference between the slopes other than as a rough measure of the uncertainty of the data is therefore not justified.

Knapp et al.[4] have measured the temperature dependence of the KIE for two additional mutants, L546A and L754A, with mutations near the reactive center that will tend to widen the pocket. The mutants have rate constants that are smaller by $2-3$ orders of magnitude than the wild-type rate constants but have similar KIEs with essentially the same temperature-dependence. This indicates that the proton transfer step is not significantly affected by the mutations and that the reason for the reduced activity should be sought elsewhere. The relevant kinetic parameters taken from this work[3,4] are collected in Table 1.

3. CH-Bond Cleavage by Methylamine and Aromatic Amine Dehydrogenase

The second system to be considered is the oxidative demethylation of primary amines to form aldehydes and ammonia catalyzed by methylamine and aromatic amine dehydrogenase (MADH and AADH). In these reactions, studied by Scrutton and co-workers,[5−7] proton abstraction by an active-site base from an iminoquinone intermediate is accompanied by electron transfer to a tryptophylquinone cofactor. Although the basic motif, proton transfer from a CH bond to an oxygen lone pair driven by electron transfer, is the same as that for SLO1, the mechanism involves two intermediate steps, namely addition of the primary amine to one of the two carbonyl groups of the quinone, followed by elimination of a water molecule and iminoquinone formation. From the observed KIEs in the range $5-20$, the authors concluded that the subsequent proton abstraction is rate-determining. The rate constants of these reactions at room-temperature cover a range of $1-10^3$ s^{-1} and are subject to activation energies in the range $10-15$ kcal/mol, but the KIEs show a weak to very weak temperature dependence. A summary of the data is listed in Table 1.

Of the two MADH substrates probed, ethanolamine shows the lower rate and the stronger temperature dependence of the KIE. The other substrate, methylamine, exhibits more complicated kinetics that deviates from the standard Michaelis−Menten scheme. Specifically, the analysis leads to rate constants for

TABLE 1: Kinetic Parameters (T in K, k in s^{-1}, E_a, the Arrhenius Activation Energy, in kcal/mol) Used in the Analysis of Temperature-dependent Kinetic Isotope Effects in (model) Enzymes[a]

Nr.	reactant(s)	T	ΔT	k^H	E_a^H	ln KIE(T)	d ln KIE/dT^{-1}	ref
1a	Linoleic acid/SLO1	298	40	401	1.7 ± 0.3	4.4	2.4	4
1b	Mutant I553A	298	40	302	1.9 ± 0.4	4.6	5.7	4
1	1a+1b	298	40	293	1.9 ± 0.2	4.5	3.2	4
2	Mutant L546A	298	40	1.28	4.0 ± 0.2	4.7	2.7	4
3	Mutant L754A	298	40	0.18	3.7 ± 0.4	4.7	2.8	4
4	Ethanolamine/MADH	298	35	14	10.4	2.8	2.6	6
5	Methylamine/MADH	298	35	175	11.3	2.8	0.6	5
6	Dopamine/AADH	298	35	132	12.1	2.6	0.4	6
7	Benzylamine/AADH	298	35	1.81	16.3	1.6	0.3	6
7a	Tryptamine/AADH	277		503	12.5	4.0		6
8	DiCu(Bn_3)complex	233	40	3.55(−3)	13.5	3.7	2.7	11

[a] The SLO1 parameters are derived from least-square Arrhenius fits to the data reported in the Supporting Information of ref 4 and differ slightly from the data listed in Table 1 of that paper.

complex formation k_{form} and dissociation k_{diss} that are isotope-dependent: $k^H_{form}/k^D_{form} = 6.4$ and $k^H_{diss}/k^D_{diss} = 19$, values comparable to the KIE for the hydrogen transfer step. As the authors recognized,[5] it follows that the KIEs reported for the proton-transfer steps, along with their temperature dependence, may be inaccurate.

Recently, Faulder et al.,[19] Alhambra et al.,[20] and Tresadern et al.[17] reported calculations aimed at modeling the proton-transfer reaction for methylamine by transition state theory with semiclassical tunneling corrections in the small-curvature approximation.[18] In the calculations, the proton transfer was treated as a one-step adiabatic process. The KIE at fixed temperature was well reproduced, but the problem of its apparent lack of temperature dependence was not addressed. However, as pointed out above, the significance of the reported experimental KIE and its temperature dependence is in doubt because of problems with the kinetic analysis of the data.

As shown in Table 1, the three AADH substrates probed[6] show a range of rate constants and KIEs such that the faster the reaction the larger its KIE. For tryptamine, a rate constant of 500 s^{-1} and a KIE of 55 was measured at 277 K, measurements at higher temperatures being outside the range of the stopped-flow technique. At the other end of the range, the corresponding values at 298 K for benzylamine are 1.8 s^{-1} and 4.8. Values for dopamine at 298 K (130 s^{-1} and 13) are intermediate. No values for k_{form} and k_{diss} are given for the enzyme−substrate complexes, but the corresponding equilibrium constant shows a small isotope effect for benzylamine, a modest isotope effect for dopamine, whereas that for tryptamine differs from unity but could not be measured quantitatively.

The authors[6] point out that these results are anomalous since it is well-known that standard one-dimensional tunneling barriers, e.g., the inverse parabola or the Eckart barrier, lead to an inverse relationship between the rate of transfer and the KIE. They offered a qualitative interpretation in terms of unusually shaped barriers with "shoulders" that would have to vary from substrate to substrate. However, they did not verify by calculation that the proposed barrier shapes would indeed have the desired effect. Moreover, it is difficult to see why barriers for simple tunneling reactions should have shoulders unless there are unstable or metastable intermediate configurations. Such configurations, which may occur in the case of multistep reactions, have not been encountered in the calculations on proton abstraction in the methylamine-MADH complex.[19,20] However, the authors' suggestion of a complex barrier shape begs the question whether such a shape might arise through kinetics more complex than considered in the analysis. In the proposed reaction mechanism, the reversible formation of the enzyme−substrate complex is followed by two presumably irreversible steps prior to proton transfer. If the rate constant of at least one of these steps is not very fast on the time scale of the proton-transfer step, the observed rate constant will involve at least two barriers, which in a simplified reaction scheme may appear as a single "fused" barrier with a complex shape. We return to this problem after analyzing the temperature dependence of the KIEs.

To account for the vanishing temperature dependence of the KIE, the authors[7] propose that the dynamics of the promoting modes (the modes causing oscillations of the barrier in their picture) remains frozen in time during the tunneling event. However, this argument does not work because the thermally averaged amplitude of these modes and thus the proton-transfer distance will be a function of temperature.[4,10,12,13] It is well-known and easily verified by the methods used in the next section that a promoting mode makes the KIE temperature-dependent at temperatures where this mode can be thermally excited. Since the measurements are carried out at room temperature, only promoting modes with frequencies above 800 cm^{-1} can be considered temperature-independent.

4. Theoretical Models for the KIE

To investigate the relationship between the KIE and its temperature dependence for models relevant to enzymatic CH cleavage, we start with the Golden Rule but allow for higher-order distortions of the vibrational potentials by including anharmonicity through the use of Morse potentials. Specifically, we assume that an increase in the coupling increases the anharmonicity and decreases the separation of the two potentials. In the Golden Rule formulation, the rate constant of a transition between two electronic states is given by

$$k(T) = (2\pi/\hbar)J^2 \sum_{i,f} |S_{fi}|^2 e^{-\epsilon_i/k_BT}\, \delta(\epsilon_f - \epsilon_i) / \sum_i e^{-\epsilon_i/k_BT} \quad (1)$$

where i and f denote collective vibrational quantum numbers for the initial and final state, respectively, and ϵ are vibrational energies and the delta function restricts the reaction to transfer between levels of the same energy. For semiquantitative purposes, we have written the interaction between the two states in the Condon approximation, separating the electronic integral J from the vibrational overlap integral S. The rate constant is governed by S^2, the Franck−Condon factor, which, in the example of section 2, will be dominated by the overlap between a methylene CH-stretch vibration and a hydroxyl OH-stretch vibration, since these vibrations combine to yield the largest vibrational displacement occurring during the reaction. The tunneling vibration is a high-frequency hydrogen stretching mode, whose thermal excitation at room temperature will be weak but whose overlap will be strongly isotope dependent. There will be other, lower-frequency vibrations that are displaced by the transfer, but these will be isotope-independent and thus will not affect the KIE; these include modes that cause the familiar Levich−Dogonadze−Marcus type reorganization effect. However, the KIE is affected indirectly by modes that involve the atoms between which the proton is transferred. These modes modulate the distance between the two overlapping hydrogenic wave functions and their thermal excitation effectively reduces this distance, thus increasing the overlap and decreasing the KIE. Their normal coordinates can be divided into two groups, depending on whether they are approximately parallel or perpendicular to the transfer path. It can be shown that the effect of the perpendicular modes is much weaker than that of the parallel modes, as expected, so that we need only consider the parallel modes. Elsewhere,[21] we have shown that they can be treated in the form of a single effective mode, whose frequency and effective mass can be derived from the vibrational force field. Since such a force field is not available in the case at hand, these properties will enter the model as parameters, along with the parameters of the tunneling mode.

The first set of model calculations is based on Morse oscillators to represent the tunneling mode and harmonic oscillators to represent the promoting mode and follow an approach we introduced earlier.[12] In this approach, which treats both motions quantum-mechanically and allows thermal excitation of both, the overlap integral between tunneling mode levels v and w is written in the form

$$S_{VW,vw} = \langle V(Y)|s_{vw}(R_0 - 2\xi + Y)|W(Y)\rangle \quad (2)$$

where V and W are promoting mode levels, 2ξ is the sum of the C−H and O−H bond lengths, and R_0 is the C−O distance. $Y = R - R_0$ is the instantaneous amplitude of the effective mode, and $R_0 - 2\xi + Y = R - 2\xi \equiv r$ is the instantaneous proton transfer distance. These matrix elements are readily evaluated numerically;[12] squared and summed, after each term is multiplied by a line shape function and a Boltzmann factor, they yield the rate constants $k(T)$ of eq 1 and KIEs in the form $\eta(T) \equiv k_H(T)/k_D(T)$. The line shape function gives the term a weight according to the distance of the final-state level from exact resonance and the Boltzmann factor gives it a weight according to the thermal population of the initial-state level. It is well-known that an Arrhenius plot of ln $k(T)$ against T^{-1} calculated in this way shows curvature if the temperature interval is large but apparent linearity if it is small as in the present experiments. The same will apply to the KIE, so that d ln η/dT^{-1} should be independent of temperature for the reactions at hand. This suggests probing the relation between the KIE and its temperature dependence by plotting d ln η/dT^{-1} against T ln η or, more conveniently, of T^{-1}d ln η/dT^{-1} = d ln η/d ln T^{-1} against ln η. Typical results are displayed as solid curves in Figure 2. For transfer distances governed by van der Waals radii with anharmonicities typical of unperturbed CH_2 and OH_2 groups, the curve is almost universal, i.e., independent of the model parameters for the range of temperatures and KIEs represented by the experiments.

To account for the shape of the curves in Figure 2, we neglect thermal excitation of the tunneling mode, i.e., we replace $s_{v w}$ in eq 2 by s_{v0}. Rate constants for endothermic reactions we obtain by multiplying the rate constant for the reverse exothermic reaction by a Boltzmann factor; this does not affect the KIE. We also approximate the line shape function by a constant ρ. Then the rate constant (1) takes the form $k(T) = (2\pi/\hbar)$-$J^2\rho S_{v0}^2(T)$, $S_{v0}^2(T)$ being the overlap s_{v0}^2, averaged over the equilibrium distribution $P(R, T) = [\sqrt{\pi}A(T)]^{-1}\exp\{-[(R - R_0)/A(T)]^2\}$:

$$S_{v0}^2(T) = \frac{1}{\sqrt{\pi}A(T)}\int \mathrm{d}R\, s_{v0}^2(R - 2\xi)\mathrm{e}^{-[(R-R_0)/A(T)]^2} \quad (3)$$

where

$$A^2(T) = A_0^2 \coth\frac{\hbar\Omega}{2k_BT} \quad (4)$$

M and Ω being the effective mass and frequency of the promoting mode, so that $A_0 = (\hbar/M\Omega)^{1/2}$ is the zero-point amplitude. We then obtain for the KIE (quantum numbers omitted)

$$\eta(T) = S_H^2(T)/S_D^2(T) \quad (5)$$

Thus, to analyze the KIE and its temperature dependence qualitatively, we only need to consider the vibrations contributing to the overlap described by eqs 3 and 4.

For a tunneling potential consisting of two crossing parabolas, the one-dimensional overlap integral s_{v0} in eq 3 can be evaluated analytically. For a near-thermoneutral reaction, we may limit ourselves to tunneling to the ground level $v = 0$ for which

$$s_{00}^2(r) = \mathrm{e}^{-r^2/2a_0^2} \equiv \mathrm{e}^{-r^2m\omega/2\hbar} \quad (6)$$

where m and ω are the effective mass and frequency of the tunneling mode, so that a_0 is the zero-point amplitude for the light isotope. Since thermal excitation of the tunneling mode is neglected, we can reintroduce anharmonicity in this expression by replacing a_0 by an effective value $a_{eff} > a_0$, chosen so that it reproduces the value calculated for the Morse potential. This approximation reduces eq 3 to

$$S_{00}^2(T) = \sqrt{\frac{2a_{eff}^2}{2a_{eff}^2 + A^2(T)}}\mathrm{e}^{-(R_0-2\xi)^2/[2a_{eff}^2+A^2(T)]} \quad (7)$$

where $A(T)$ is the only factor that depends on temperature. This result illustrates the promoting effect of the donor−acceptor motion, as $S_{00}^2(T)$ can be represented in the form of the overlap (6), $S_{00}^2(T) \equiv \mathrm{e}^{-r_0^2(T)/2a_{eff}^2}$, but with a temperature- and isotope-dependent effective tunneling distance $r_0(T)$ which is shorter than r_0 as follows from

$$r_0(T) = \frac{r_0}{\sqrt{1 + A^2(T)/2a_{eff}^2}}. \quad (8)$$

The overlap and the effective tunneling distance become temperature-independent when thermal excitation of the promoting mode can be neglected, namely in the limit $\hbar\Omega \gg 2k_BT$, where $A^2(T) \rightarrow \hbar/M\Omega$. For the present purpose, the inequality sign $\gg$ may be interpreted as >2 or $\Omega > 800$ cm^{-1}. In the opposite limit, $\hbar\Omega \ll 2k_BT$, we can approximate $A^2(T)$ by $2k_BT/M\Omega^2$, which thus depends only on the force constant of the skeletal promoting mode $k_s = M\Omega^2/2$. This allows us to derive the following simple relations for the KIE and its temperature dependence for $a_{0,D}^2 = a_{0,H}^2/\sqrt{2}$ and temperatures such that $\hbar\Omega \leq 0.5k_BT$:

$$\ln C\eta = \frac{2a_{eff}^2 r_0^2(\sqrt{2} - 1)}{[2a_{eff}^2 + A^2(T)][2a_{eff}^2 + A^2(T)\sqrt{2}]} \quad (9)$$

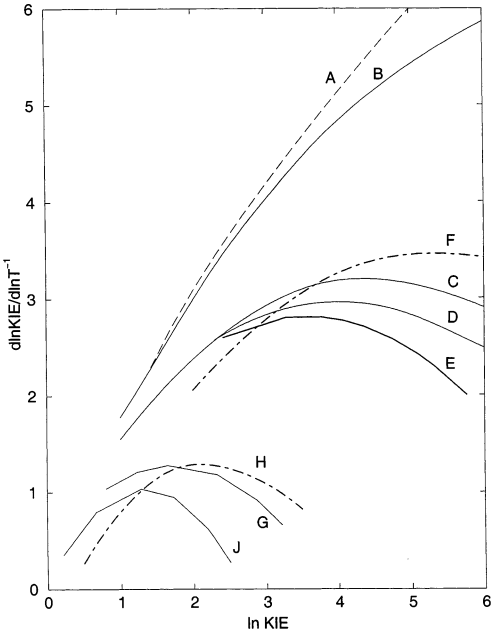

Figure 2. General relationship for the temperature dependence of kinetic isotope effects calculated for a two-oscillator model, in which the tunneling potential is represented by two crossing parabolas or Morse curves or a quartic potential, and the promoting-mode potential is harmonic. The curves are calculated for a tunneling-mode frequency $\omega^H/\omega^D = 3000/2150$ cm^{-1} together with the parameter values listed in Table 2 by varying the temperature and the force constant of the promoting mode.

$$\frac{1}{T}\frac{\mathrm{d}\ln C\eta}{\mathrm{d}T^{-1}} = 2\ln C\eta - \frac{4a_{\mathrm{eff}}{}^2 + (\sqrt{2}+1)A^2(T)}{(\sqrt{2}-1)r_0{}^2}\ln^2 C\eta \quad (10)$$

where $r_0 = R_0 - 2\xi$ is the equilibrium transfer distance and

$$C = \sqrt{\frac{2a_{\mathrm{eff}}{}^2 + A^2(T)}{2a_{\mathrm{eff}}{}^2 + A^2(T)\sqrt{2}}} \quad (11)$$

varies between 1 if $2a_{\mathrm{eff}}{}^2 \gg A^2(T)$ and 0.84 if $2a_{\mathrm{eff}}{}^2 \ll A^2(T)$; for qualitative purposes it can be set equal to unity.

Equation 10 is a new result, which links the temperature dependence of the KIE in the form d ln KIE/d ln T^{-1} directly to ln KIE, given by eq 9. The relationship consists of a linear term, which is independent of model parameters, including the temperature, and a quadratic term governed by the vibrational amplitudes a_{eff} and $A(T)$, and the proton-transfer distance r_0. The advantage of this representation is that it leads to a universal curve under "normal" conditions, i.e., tunneling distances governed by van der Waals radii and temperatures sustaining biological activity. Outside this range, the quadratic term becomes important and the universal curve splits and fans out into a series of model-dependent curves. Substituting the KIE and its temperature dependence into eqs 9 and 10, one can directly obtain the ratios $A(T)/a_{\mathrm{eff}}$ and r_0/a_{eff}. The tunneling-mode amplitude a_{eff} can be estimated through, e.g., Morse potentials, for a chosen model and should be consistent with the resulting values of r_0 and $A(T)$ for that model. In this manner, these equations allow a qualitative test of a proposed transfer mechanism. In general, a_{eff} will increase with increasing anharmonicity and thus with increasing electronic coupling, leading to a corresponding increase of the transfer distance r_0 required to fit a given set of KIE data.

The parabolic curves predicted by eq 10 rationalize the plots in Figure 2 obtained numerically by the method of ref 12, which is more general than the model used to derive the equation, as it includes thermal excitation of both the tunneling mode and the promoting mode, as well as numerical evaluation of the overlaps (2). The solid curves in Figure 2 are calculated for Morse-type (B−E,G,J) tunneling modes with the broken curve (A) representing the harmonic limit. Parameter values, to be discussed in the next section, are listed in Table 2. For small KIE values, the increase of d ln KIE/d ln T^{-1} with ln KIE is governed by the linear term of eq 10 and will thus be model-independent unless the transfer distance is very small. For larger KIEs, the quadratic term, which reduces the temperature dependence, becomes important. Its coefficient is of the same form as $1/\ln S_{00}{}^2(T)$, $S_{00}{}^2(T)$ being the two-dimensional squared vibrational overlap integral (7). Large KIEs that are weakly dependent on temperature can occur only when the force constant of the promoting mode is very large. To show this, we rewrite eq 10 in the form

$$\frac{1}{T}\frac{\mathrm{d}\ln C\eta}{\mathrm{d}T^{-1}} = \left[2 - \frac{2a_{\mathrm{eff}}{}^2}{2a_{\mathrm{eff}}{}^2 + A^2(T)} - \frac{2a_{\mathrm{eff}}{}^2}{2a_{\mathrm{eff}}{}^2 + A^2(T)\sqrt{2}}\right]\ln C\eta \quad (12)$$

It follows that the term in square brackets will be small if $A(T)$ is small and thus if the corresponding force constant is large. In general, this will require strong hydrogen bonding along the proton-transfer path.

TABLE 2: Fixed Parameters Used to Calculate the Curves Displayed in Figures 2 and 3[a]

	Figure 2				Figure 3			
letter	type	r_0	X	$\lvert\Delta E\rvert$	type	r_0	X	$\lvert\Delta E\rvert$
A	harmonic	1.3	0/0		Morse	1.3	30/15	
B	Morse	1.3	60/30		Morse	1.0	100/50	10
C	Morse	0.9	60/30		Quartic	0.9		
D	Morse	0.9	100/50		Quartic	0.6		
E	Morse	0.9	100/50	4	Quartic	0.5		
F	Quartic	1.0						
G	Morse	0.6	150/75					
H	Quartic	0.6						
J	Morse	0.6	150/75	4				

[a] The transfer distance r_0 is expressed in Å, the (negative) anharmonicity $X^{\mathrm{H}}/X^{\mathrm{D}}$ in cm^{-1}, and the exo(endo)thermicity $\pm\Delta E$ in kcal/mol.

If the transfer is sufficiently exothermic or endothermic for transitions to or from the $v = 1$ level of the tunneling mode to become dominant, the integral s_{00} in eq 3 is replaced by the corresponding integral s_{10}. This will increase the value of a_{eff} and thus of the quadratic term in eq 10. Note that exo- and endothermicity will have the same effect on the overlap integral and thus also on the KIE, but of course not on the rate constant. This exo- or endothermicity will affect the relationship between the KIE and its temperature dependence only when the quadratic term is important, in which case its effect will be similar to that of reducing the transfer distance. These effects are also illustrated in Figure 2.

For short transfer distances and low barriers, the derivation needs to be modified. To represent this situation, we have performed a second series of calculations based on the adiabatic approximation. Instead of two crossing Morse potentials interacting through a coupling term, we use a single double-minimum potential to describe the motion of the proton in the collinear heavy-light-heavy particle system and allow modulation of the height and width of the corresponding barrier by a promoting mode. To illustrate such a system, we use a simple quartic potential of the form

$$U(x, Y) = p(Y)x^4 - q(Y)x^2 \quad (13)$$

where $Y = R - R_0$ is a harmonic promoting-mode coordinate. Like the harmonic potential this quartic potential is governed by only two parameters, which we take to be ω, the frequency in the well, and r_0, the barrier width. The dot−dash curves (F,H) corresponding to this potential for the variable parameter values listed in Table 2 have been evaluated numerically within the semiclassical instanton framework.[22,23] They show the same general behavior as the curves calculated for crossing Morse potentials with suitably adjusted anharmonicities, despite the fact that the former uses an adiabatic and the latter a nonadiabatic approach.

When $A(T)$ can be approximated by its high-temperature value, this approach leads to equations of the same form as eqs 9 and 10 but with a different coefficient for the quadratic term, namely[23]

$$\ln\eta = \frac{a_0{}^2 r_0{}^2(\sqrt{2}-1)}{3\left[a_0{}^2 + \frac{1}{4}A^2(T)\right]\left[a_0{}^2 + \frac{1}{4}A^2(T)\sqrt{2}\right]}; \quad (14)$$

$$\frac{1}{T}\frac{\mathrm{d}\ln\eta}{\mathrm{d}T^{-1}} = 2\ln\eta - 3\frac{2a_0{}^2 + \frac{1}{4}(\sqrt{2}+1)A^2(T)}{(\sqrt{2}-1)r_0{}^2}\ln^2\eta \quad (15)$$

for $C = 1$, where $a_0 = (\hbar/m\omega)^{1/2}$, the zero-point energy of the light isotope, ω being the curvature at the bottom of the wells. Just as eqs 9 and 10, eqs 14 and 15 represent results that are more approximate than the plotted curves.

5. Model Parameters

The properties of the tunneling mode are governed by its frequency ω, anharmonicity X, reduced mass m, transfer distance r_0, as well as the asymmetry of the barrier represented by the exothermicity $-\Delta E$. We set $\omega^H = 3000$ cm^{-1}, $\omega^D = 2150$ cm^{-1}, $m^D = 2m^H = 2$, so that the harmonic zero-point amplitude a_0 will be 0.105 Å for H and 0.089 for D; we retain X, r_0, and ΔE as variable parameters. From the van der Waals radii of the methylene and hydroxyl groups, we estimate a proton-transfer distance $r_0 \geq 1.3$ Å, where the lower limit corresponds to a collinear arrangement. The anharmonicity of an isolated CH- or OH-stretch fragment amounts roughly to $X = -60$ cm^{-1}.[24] This leads to a normal-mode anharmonicity of about half that value for CH_2 and OH_2 groups. However, if a specific proton is engaged in hydrogen bonding, much larger anharmonicities may be expected along with shorter transfer distances. For the exo- or endothermicity, we take three values in the experimental range,[1−7] namely 0, 4, and 10 kcal/mol.

The only promoting-mode properties that enter as variable parameters are the reduced mass M and the frequency Ω, along with the temperature T. In the temperature ranges of interest, they can be approximately treated together as the single continuous variable $A^2(T)$. The curves in Figure 2 that are based on harmonic and Morse potentials are calculated by the method of ref 12; those based on quartic potentials are calculated by an equivalent numerical procedure within the instanton framework.[23] In the actual calculations, Ω is varied for chosen values of the other parameters.

The top pair of curves is calculated for a transfer distance of 1.3 Å, corresponding to the minimum van der Waals distance. The harmonic curve (A) is almost linear. The Morse curve (B), calculated for an anharmonicity $X = -60$ cm^{-1}, is slightly bent but turns out to be virtually invariant for reasonably small variations of the other parameters, including the exo- or endothermicity, for KIE values up to 100, as the linear term of eq 10 remains dominant. Morse curves calculated for anharmonicities smaller than 60 cm^{-1} are intermediate between this curve and the harmonic curve. Since these curves thus depend only on the transfer distance, it follows unequivocally that a large KIE with a vanishing temperature dependence is incompatible with such a large transfer distance, independent of the transfer model chosen. This confirms and generalizes the results of recent model calculations of Knapp et al.[4]

The middle group of curves corresponds to a transfer distance of about 1 Å and represents the case of weak to moderately strong hydrogen bonding. At these distances, the quadratic term of eqs 10 becomes important for KIE values higher than 20, so that the upper part of the curve will exhibit some dependence on parameters other than the transfer distance and the anharmonicity, especially the endothermicity, if any. The thin solid curves shown are calculated with the Morse-oscillator model for a transfer distance of 0.9 Å, tunneling-mode anharmonicities $X = -60$ (C) and -100 cm^{-1} (D), and a thermoneutral transition. The effect of an exo- or endothermicity of 4 kcal/mol on the curve calculated with $X = -100$ cm^{-1} is shown by the thick solid line (E). Comparison of these curves shows that the effect of an exo- or endothermicity of 4 kcal/mol is comparable to that of an increase in anharmonicity from -60 to -100 cm^{-1}. The dot−dash curve (F) is calculated for a quartic potential with a transfer distance of 1.0 Å and a frequency of 3000/2150 cm^{-1} at the bottom of the well.

The bottom curves correspond to a transfer distance of 0.6 Å, characteristic of very strong hydrogen bonding. Except for very small KIEs, the quadratic term dominates in this case, which makes the curve strongly dependent on the endothermicity and the properties of the two model vibrations. To obtain a proper representation of the corresponding potential, it is probably necessary to go beyond the Golden Rule and adopt a suitable double-minimum potential. The dot−dash curve (H) shows the result for a quartic potential, which yields a temperature dependence for the KIE similar to that of a Morse potential with an anharmonicity $X = -150$ cm^{-1} (G). Curve J shows the effect on the Morse curve of an exo- or endothermicity of 4 kcal/mol.

6. Applications

6.1. Lipoxygenase. The rate constants of the SLO1 reaction, studied by Klinman et al.,[3,4] listed along with the relevant kinetic parameters in Table 1, indicate slow proton transfer consistent with a transfer distance close to the expected van der Waals separation of the donor and acceptor groups. The reported activation energy of about 2 kcal/mol is in line with values observed for proton tunneling assisted by thermally excitable skeletal vibrations. However, it does not account for the substantial reorganization factor (Franck−Condon contribution) expected to accompany proton transfer. Since for the present system the reorganization energy can easily amount to several kilocalories per mol, the absence of substantial thermal activation indicates that the results correspond to the "inverted regime" of the standard Levich-Dogonadze-Marcus model characterized by a reorganization energy smaller than the exothermicity $-\Delta E$. For that regime, the temperature dependence of the Franck−Condon contribution is usually small. The estimate $\Delta E = -6$ kcal/mol of Knapp et al.[4] implies that the Franck−Condon factor generated by this reorganization is unlikely to cause a substantial reduction of the transfer rate and thus supports the notion of a relatively large transfer distance.

However, attempts to model the observed KIE and its temperature dependence led to transfer distances of 0.6−0.7 Å,[4] about half the value expected on the basis of van der Waals radii. Introduction of Morse potentials with anharmonicities up to 60 cm^{-1} boost these values to 0.7−0.8 Å, which does not solve the problem. The corresponding promoting mode frequencies are in the range 220−280 cm^{-1} for a reduced mass of 25, their high value being the reason for the reduced temperature dependence of the KIE. Clearly, the corresponding force constant is abnormally high for a complex bound by van der Waals forces.

One way to account for the short transfer distances and the large promoting-mode force constant is to assume that the adjacent strong redox system induces an attractive force in the form of a hydrogen bond between the donor CH_2 and acceptor OH groups. Such a force would reduce the distance and increase the anharmonicity. In Figure 3, the SLO1 data points labeled 1−3 are shown to fit a Morse curve (B) calculated for a distance of 1.0 Å, an anharmonicity of 100 cm^{-1} and $\Delta E = -10$ kcal/mol, as well as a quartic curve (C) calculated for the distance 0.9 Å. In both cases, the promoting mode frequency is of the order of 175 cm^{-1} for a reduced mass of 25. Point 1 is derived from the combined data sets of the wild-type enzyme and the I553A mutant, based on the assumption, supported by Table 1 of ref 4, that the mutation has a negligible effect on the efficiency of the enzyme. As shown in Figure 1 and discussed

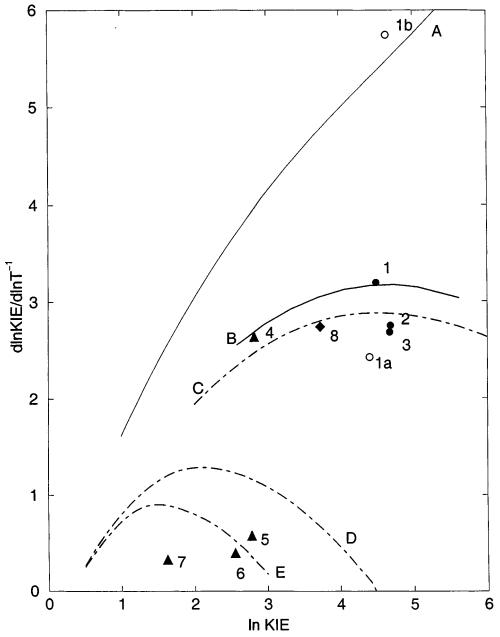

Figure 3. Comparison of experimental data points for enzymatic (model) reactions with the model relation of Figure 2. The points and the corresponding data are listed in Table 1. The parameter values appropriate to the curves are listed in Table 2.

in section II, combining the two data sets yields more consistent correlation coefficients for the Arrhenius plots and is thus statistically justified. If the two data sets are taken separately, point 1 is replaced by point 1a for the wild-type enzyme and point 1b for the mutant; their large vertical separation reflects the low correlation coefficients of the Arrhenius plots. Points 2 and 3 in Figure 3 are derived from the data sets of the L546A and L754 mutants, respectively. They are close to point 1 (and point 1a), which indicates that the tunneling step is essentially the same for the four (or three) species. Taken separately, point 1b would fit a model that combines a standard van der Waals transfer distance of 1.3 Å with a normal methylene group anharmonicity of 30 cm^{-1}, illustrated by curve A in Figure 3. However, this interpretation is contradicted by the observation that this mutant is as efficient as the wild-type enzyme. It also fails to account for the presence of the strong redox group.

In view of the paucity of data, we do not attempt to assign error limits to individual points. The low correlation coefficients of the Arrhenius plots discussed in section II indicate that the uncertainties are large and leave room for fitting parameters, especially tunneling distances, substantially different from those obtained above. However, the observation that the points 1−3 in Figure 3 all cluster around curves representing a tunneling distance of 0.9−1.0 Å supports the general observation that the temperature dependence of the KIE cannot be explained on the basis of a tunneling distance governed by van der Waals radii. Instead, it suggests that the hydrogen transfer takes place along a path shortened by the formation of a hydrogen bond.

The appearance of hydrogen bonding assigns a specific role to the redox system, namely electron withdrawal from the methylene group of the substrate. To assess the extent of this withdrawal and its effect on the initial, transition and final states, quantum-chemical calculations will be required. The effect should be large enough to turn the natural repulsion between a methylene group and a water molecule into attraction based on hydrogen bonding but not so large as to cause very rapid transfer. The given fitting parameters represent a compromise that is suitable to reproduce the observed KIEs and their temperature dependence. Whether they remain appropriate with respect to the observed rate constants cannot be established without a quantum-chemical evaluation of the transfer potential.

6.2. Methylamine and Aromatic Amine Dehydrogenase. The rate constants of the reactions catalyzed by MADH and AADH are thermally activated as indicated by the activation energies reported by Scrutton et al.[5−7] and listed in Table 1. These activation energies are considerably larger than those normally encountered in exothermic proton tunneling and those observed for SLO1 and its mutants. This indicates that proton transfer is either endothermic or subject to a large reorganization energy, which, according to the standard Levich−Dogonadze−Marcus model, would give rise to a very small and temperature-dependent Franck−Condon factor in the "normal regime". No error bars or correlation coefficients for the temperature-dependence of the rate constants are reported but the published Eyring plots indicate correlation coefficients >0.99, i.e., values very much higher than those reported in ref 4. The description of the measurements and procedures in ref 4−7 sheds no light on this apparent discrepancy.

Among the five amine substrates for which KIEs are reported, ethanolamine stands out because its KIE shows by far the largest temperature dependence. It gives rise to the point labeled 4 in Figure 3, which fits the same curves (B,C) as the lipoxygenase points 1−3. This means that the same values for the tunneling distance and the anharmonicity apply, with the main difference being a smaller value for the force constant of the promoting mode, which can be represented by a frequency of about 135 cm^{-1} for a reduced mass of 25.

Although the temperature dependence of the KIE of the ethanolamine reaction indicates a transfer distance similar to that derived for SLO1, that of methylamine yields a much smaller distance. If we ignore the observed anomalous isotope dependence of the formation and dissociation constants of the enzyme−substrate complex and accept the rate constants reported for methylamine at face value, we obtain the point labeled 5 in Figure 3. It corresponds to a proton-transfer distance of 0.6−0.5 Å for a quartic potential (curves D and E) and thermoneutral proton tunneling. Under these conditions, the promoting-mode force field corresponding to the observed KIEs is strong as expected for strong hydrogen bonding. An appropriate value for the reduced mass may be about 10, leading to a promoting-mode frequency of about 500 cm^{-1}. This situation leads to very rapid tunneling with rate constants estimated to be $>10^{10}$ s^{-1} for "reasonable" parameter values. If the proton transfer is endothermic or, in a two-step process, exothermic, slightly longer transfer distances are obtained, but no reasonable combination of parameter values can raise it to a distance that would make it compatible with our model. Although the transfer rate is higher for methylamine than for ethanolamine, the difference is much smaller than expected on the basis of the difference in transfer distance deduced from the KIEs.

The series of three substrates catalyzed by AADH, discussed in section III, shows an anomalous relationship between the rate constants and the KIEs. The increase of the KIE in the order benzylamine < dopamine < tryptamine indicates a corresponding increase of the barrier width and/or height. However, the corresponding reduction in the rate constant expected for a one-step process is not observed. On the contrary, the rate constants *increase* in this order. To account for this apparent anomaly on the basis of one-step electron−proton tunneling, we would have to make the unreasonable assumption that the reorganization factor increases inversely proportional to the width of the barrier. The actual values of the KIE vary from 5 for benzylamine to

50 (at 277 instead of 298 K) in tryptamine. Temperature-dependent KIEs are available for benzylamine and dopamine and are represented by points 6 and 7 in Figure 3. These points are close to point 5 representing methylamine and correspond to a transfer distance of at most 0.6 Å for a quartic potential.

The corresponding tunneling potentials lead to transfer rate constants at least 8−10 orders of magnitude larger than the observed values in the range 2−500 s^{-1}. This would imply that the transfer is subject to very small Franck−Condon factors corresponding to large reorganization energies. These would be temperature-dependent and may account for the observed activation energies. The fact that the largest activation energy is observed for benzylamine, which has the smallest rate constant, is consistent with this interpretation. However, the reorganization energy should be basically isotope-independent and therefore cannot explain the observed variation in the KIE among the three substrates.

It follows that the methylamine and AADH data cannot be explained by the present model for proton tunneling in which tunneling is assisted by a promoting mode and suppressed by a reorganization factor. This failure may be due to problems with the model or problems with the data. Because the model includes all recognized physical effects on tunneling in a complex environment, it is not clear how to improve it in ways that might lead to elimination of the large discrepancy. Therefore, we focus here on the possibility that there are problems with the experimental data.

As pointed out in section III, the kinetics is more complicated than that of SLO1 and involves three presumably separate steps following complex formation, the last of these steps being proton transfer. The kinetic analysis is based on the assumption that the two steps preceding proton transfer are fast and irreversible. For methylamine, this assumption leads to unacceptably large kinetic isotope effects on the rates of complex formation and dissociation and an unexplained relationship of its rate constant with that of ethanolamine. For the AADH substrates probed, no rate constants of the processes preceding proton transfer are available, but small kinetic isotope effects on the corresponding equilibrium constants are observed. The rate constants and KIEs of these substrates show an anomalous correlation, which has been qualitatively interpreted by the authors in terms of a "compound" barrier, such as may be expected to arise if a compound reaction is described in terms of a single reaction coordinate. We believe these anomalies cast reasonable doubt on the validity of a kinetic analysis in terms of a simple rate-determining proton-transfer step.

We therefore offer the suggestion that the rate constants observed for these substrates reflect the influence of kinetic steps prior to proton tunneling. Specifically, we suggest that proton transfer is essentially rate-determining in tryptamine and that a preceding heavy-atom reaction is essentially rate-determining in benzylamine, with dopamine representing an intermediate situation. This would allow the assumption that the intrinsic, as opposed to the observed, KIE is roughly the same for the three substrates and that the different rate constants are mostly due to the preceding steps. It would also offer a qualitative explanation for the very weak temperature dependence of the KIE in benzylamine and dopamine as due to the reduced contribution of the tunneling step to the observed rate constant. A similar argument is proposed for methylamine; whether this can eliminate the anomalous isotope effects on the equilibrium constant of the complex cannot be judged on the basis of the available data.

6.3. Dicopper Complexes. To further test possible effects of the protein environment on the hydrogen-transfer distance in enzymatic CH-bond cleavage, we have extended the study to systems representing reactive centers outside a protein framework. Many enzymes (monooxygenases) are known in which the active site contains copper complexes that bind and activate dioxygen such that it abstracts a hydrogen from an alkyl group. Bis(μ-oxo)dicopper complexes have been synthesized that model this reaction by abstracting a hydrogen from an N-alkyl copper ligand.[11] Prior to or simultaneous with the proton abstraction, an electron is abstracted from an N-alkyl copper ligand, which reduces Cu^{III} to Cu^{II}. The proton transfers to one of the two oxygen atoms that bridge the copper ions. Hence, this mechanism closely resembles that of SLO1 and MADH, but operates in a valence-bound compound. This model reaction not only avoids the kinetic complications inherent in enzyme−substrate complexation but also avoids being subject to protein dynamics.

The kinetic data quoted in Table 1 refer to the complex with three benzyl ligands[11] and are derived from Arrhenius plots with correlation coefficients of about 0.997. They show that the proton-transfer reaction in the complex, measured in methylene chloride at temperatures in the range 213−263 K, exhibits a KIE that is large (about 40 at 233 K) but depends only weakly on temperature, a pattern very similar to the KIEs observed for the enzymatic reactions discussed above. Comparison with these reactions indicates that the activation energy of about 13.5 kcal/mol cannot be solely due to the tunneling process unless this process is strongly endothermic. In Figure 3, the corresponding data point labeled 8 fits model curves B and C, similar to those found appropriate for the linoleic acid and ethanolamine reactions with a transfer distance of 0.9 for Morse a potential with an anharmonicity of 100 cm^{-1} and a quartic potential. The corresponding promoting-mode frequencies are about 150 cm^{-1} for a reduced mass of 25. With these parameters, the temperature dependence of a roughly thermoneutral tunneling reaction at 233 K would contribute about 2 kcal/mol to the activation energy. The remaining 11.5 kcal/mol may be assigned to endothermicity and/or reorganization effects.

The similarity of these kinetic data to those of the enzymes suggests that the tunneling rate in the enzymes is governed by the local structure of the active site and that the effect of more distant parts of the protein is minimal. This supports the idea that in the examples cited the catalytic action of the enzyme on CH-bond cleavage is due to electron withdrawal by means of a strong redox system, leading to formation of a moderately weak hydrogen bond, which provides a suitable pathway for the transfer.

7. Conclusion

The transfer of a hydrogen atom or proton from a CH to an OH bond is a difficult process because of strong repulsion between the electrons of the CH bond and the lone-pair electrons of oxygen. The simplest way to catalyze such a process is to lower the repulsion by withdrawing electrons from the system. It is therefore reasonable to assume that evolution has chosen this route. Indeed, the examples treated in this study all contain a strong redox group in the immediate proximity of the tunneling site. Electron withdrawal has two effects: it shortens the distance between the interacting CH and OH groups and it lowers the barrier to H transfer. The corresponding tightening of the bonding between the proton donating and accepting groups increases the frequency of the dominant promoting vibration, thereby reducing the temperature dependence of the deuterium isotope effect.

Thus, according to our analysis, the appearance of enzymatic reactions that have large KIEs with a weak temperature dependence can be understood in terms of hydrogen bonding involving a CH bond. This bonding reduces a naturally high and wide barrier to a size where tunneling becomes feasible, although not easy. The situation leads to slow hydrogen transfer with a large KIE. This process is assisted by vibrations that modulate the distance between the proton donor and acceptor groups. Hydrogen bonding singles out the vibration involving the mutual motion of the donor and acceptor atoms as the most effective and gives it a frequency high enough to resist thermal excitation. Therefore, the KIE will show a weak temperature dependence. Finally, the need for hydrogen bonding explains the presence of a strong redox system in all of these systems.

In this contribution, we have modeled the resulting hydrogen bonded C···H···O system by various two-dimensional potentials, one representing the hydrogen motion between C and O and the other representing the C···O motion. From these models, we derived expressions for the KIEs and their temperature dependence. By comparing these expressions with the available experimental data, we then attempted to gain information on the structure and energetics of the reaction site.

The results of this comparison are ambiguous. The observed KIEs roughly fall into two groups. One group, which includes SLO1 and its mutants reacting with linoleic acid, MADH reacting with ethanolamine, and the dicopper complex reacting with a benzyl ligand, exhibits temperature-dependent KIEs that are consistent with the predictions of the model. In fact, all of these systems fit the same subset of curves corresponding to a proton-transfer distance of 0.9−1.0 Å together with an anharmonicity and a promoting-mode force constant consistent with hydrogen bonding. The presence of a strong redox system is assumed to account for these parameter values. The other group of data, which includes MADH reacting with methylamine and AADH reacting with benzylamine and dopamine is inconsistent with the model for physically acceptable parameter values. Specifically, attempts to fit these data yield transfer distances that are too short to allow justification by the available redox system. If it is accepted that, despite its basic simplicity, the model contains all of the interactions recognized as important for proton tunneling and that therefore it provides a useful consistency test, then the discrepancy indicates problems with the reported rate constants. This may well be the case since these rate constants are not directly observed, but derived by fitting measured (but rarely reported) curves to parameters appearing in kinetic models that at best are approximate summaries of the actual kinetics. If on the other hand it is accepted that the rate constants accurately reflect the properties of rate-determining proton tunneling steps, then a major element is lacking in our understanding of proton tunneling in a complex environment. The possibility that the missing element might be the effect of remote parts of the protein on the tunneling was considered, but no evidence was found for such an effect.

References and Notes

(1) Bahnson, B. J.; Klinman, J. P. *Methods Enzymol.* **1995**, *249*, 373.

(2) Kohen, A.; Klinman, J. P. *Acc. Chem. Res.* **1998**, *31*, 397. Kohen, A.; Klinman, J. P. *Chem. Biol.* **1999**, *6*, R191. Rickert, K. W.; Klinman, J. P. *J. Am. Chem. Soc.* **1999**, *121*, 1997. Kohen, A.; Cannio, R.; Bartolucchi, S.; Klinman, J. P. *Nature* **1999**, *399*, 496. Cha, Y.; Murray, C. J.; Klinman, J. P. *Science* **1989**, *243*, 1325.

(3) Rickert, K. W.; Klinman, J. P. *Biochemistry* **1999**, *38*, 12218.

(4) Knapp, M. J.; Rickert, K. W.; Klinman, J. P. *J. Am. Chem. Soc.* **2002**, *124*, 3865.

(5) Basran, J. B.; Sutcliffe, M. J.; Scrutton, N. S. *Biochemistry* **1999**, *38*, 3218.

(6) Basran, J. B.; Patel, S.; Sutcliffe, M. J.; Scrutton, N. S. *J. Biol. Chem.* **2001**, *276*, 6234.

(7) Basran, J. B.; Sutcliffe, M. J.; Scrutton, N. S. *J. Biol. Chem.* **2001**, *276*, 24581. Harris, R. J.; Meskys, R.; Sutcliffe, M. J.; Scrutton, N. S. *Biochemistry* **2000**, *39*, 1189.

(8) Nesheim, J. C.; Lipscomb, J. D. *Biochemistry* **1996**, *35*, 10240. Brazeau, B. J.; Wallar, B. J.; Lipscomb, J. D. *J. Am. Chem. Soc.* **2001**, *123*, 10421. Brazeau, B. J.; Austin, R. N.; Tarr, C.; Groves, J. T.; Lipscomb, J. D. *J. Am. Chem. Soc.* **2001**, *123*, 11831.

(9) Antoniou, D.; Schwartz, S. D. *Proc. Natl. Acad. Sci. U.S.A.* **1997**, *94*, 12360.

(10) Kuznetsov, A. M.; Ulstrup, J. *Can. J. Chem.* **1999**, *77*, 1085.

(11) Mahapatra, S.; Halfen, J. A.; Tolman, W. B. *J. Am. Chem. Soc.* **1996**, *118*, 11575. Only the complex with benzyl ligands is used in our analysis, since a peroxo isomer may contribute to the complex with isopropyl ligands (Tolman, W. B., private communication).

(12) Siebrand, W.; Wildman, T. A.; Zgierski, M. Z. *J. Am. Chem. Soc.* **1984**, *106*, 4083; 4089.

(13) Siebrand, W.; Smedarchina, Z.; Zgierski, M. Z.; Fernández-Ramos, A. *Int. Rev. Phys. Chem.* **1999**, *18*, 5.

(14) Smedarchina, Z.; Fernández-Ramos, A.; Siebrand, W. *J. Comput. Chem.* **2001**, *22*, 787.

(15) Benderskii, V. A.; Makarov, D. E.; Wight, C. H. *Adv. Chem. Phys.* **1994**, *88*, 1.

(16) Minor, W.; Steczko, J.; Stec, B.; Otwinowski, Z.; Bolin, J. T.; Walter, R.; Axelrod, B. *Biochemistry* **1996**, *35*, 10701. Boyington, J. C.; Gaffney, B. J.; Amzel, L. M. *Science* **1993**, *260*, 1482.

(17) Tresadern, G.; McNamara, P.; Mohr, M.; Wang, H.; Burton, N. A.; Hillier, I. H. *Chem. Phys. Lett.* **2002**, *358*, 489.

(18) Lu, D.-h.; Truong, T. N.; Melissas, V. S.; Lynch, G. C.; Liu, Y.-P.; Garrett, B. C.; Steckler, R.; Isaacson, A. D.; Rai, S. N.; Handcock, G. C.; Lauderdale, J. G.; Joseph, T.; Truhlar, D. G. *Comput. Phys. Commun.* **1985**, *17*, 235. Liu, Y.-P.; Lynch, G. C.; Truong, T. N.; Lu, D.-h.; Truhlar, D. G.; Garrett, B. C. *J. Am. Chem. Soc.* **1993**, *115*, 2408.

(19) Fauler, P. F.; Tresadern, G.; Chohan, K. K.; Scrutton, N. S.; Sutcliffe, M. J.; Burton, N. A. *J. Am. Chem. Soc.* **2001**, *123*, 8604.

(20) Alhambra, C.; Sánchez, M. L.; Corchado, J. C.; Gao, J.; Truhlar, D. *J. Chem. Phys. Lett.* **2002**, *355*, 388.

(21) Smedarchina, Z.; Siebrand, W. *Chem. Phys.* **1993**, *170*, 347.

(22) Benderskii, V. A.; Goldanskii, V. I.; Makarov, D. E. *Chem. Phys.* **1991**, *154*, 407.

(23) Smedarchina, Z., unpublished results.

(24) Herzberg, G. *Molecular Spectra and Molecular Structure. I. Diatomic Molecules*, 2nd ed.; D. van Nostrand Company, Inc.: Princeton, 1950.